

# Online Appendix: Four-set Hypergraphlets for Characterization of Directed Hypergraphs

If the preview is not legible, please download the PDF file.

## A. Datasets (Table II of the main paper)

We describe the representation, sources, and preprocessing steps of the datasets used in this work. As a default preprocessing step, we remove all duplicate hyperarcs and self-loops.

- **Metabolic datasets:** We use two metabolic datasets, `metabolic-iAF1260b`, and `metabolic-iJO1366`. Each node represents a gene, and each hyperarc represents a metabolic reaction, where each head and tail set indicates a set of genes. When the genes in the tail set participate in a metabolic reaction, they become the genes in the head set of the corresponding hyperarc. They are provided in the complete form of directed hypergraphs [1] which do not require any preprocessing step.
- **Email datasets:** We use two email datasets, `email-enron` [2], and `email-eu` [3]. Each node represents an account, and each hyperarc represents an email from a sender to one or more recipients, where the tail set consists of a node representing the sender, and the head set consists of nodes representing the recipients. We transformed the original pairwise graph into a directed hypergraph by considering all edges occurring at the same timestamp from the same sender as a single email (hyperarc). Note that the size of tail sets is always 1 in these datasets. (i.e.,  $|T_i| = 1, \forall i = \{1, \dots, |E|\}$ .)
- **Citation datasets:** We use two citation datasets from DBLP: `citation-data-science`, and `citation-software` [4], [5]. We extracted papers in the fields of data science or software from the dataset. Nodes represent authors and the (head and tail) sets indicate co-authors of each publication. Hyperarcs indicate citation relationships, with the tail set representing the paper that cites the head set paper.
- **Question & Answering datasets:** We use two question & answering datasets, `qna-math` and `qna-server`. Following [6], we created a directed hypergraph from the log data of the two question-answering sites [7]: Math Exchange and Server Fault. Each node represents a user, and each hyperarc represents a post, with the tail set consisting of the answerers and the head set consisting of the questioner. Note that the size of head sets is always 1 in these datasets. (i.e.,  $|H_i| = 1, \forall i = \{1, \dots, |E|\}$ .)
- **Bitcoin transaction datasets:** We use three bitcoin transaction datasets, `bitcoin-2014`, `bitcoin-2015`, and `bitcoin-2016`, created from the original datasets [8], as suggested in [6]. They contain the first 1.5 million transactions in Nov 2014, Jun 2015, and Jan 2016, respectively. Each node represents an individual account, and

each hyperarc represents a cryptocurrency transaction. The tail set of a hyperarc corresponds to the accounts selling the cryptocurrency, while the head set corresponds to the accounts buying the corresponding cryptocurrency.

## B. Concentration Bounds (Section IV of the main paper)

We present the sample concentration bounds of D-MoCHy and CODA-A, along with their corresponding proofs as below.

**Lemma 1** (Hoeffding's inequality [9]). *Let  $X_1, X_2, \dots, X_n$  be independent random variables with  $a_j \leq X_j \leq b_j$  for all  $j \in [n]$ . Consider the sum of random variables  $X = X_1 + \dots + X_n$ . Then for any  $t > 0$ , we have*

$$\Pr[|X - \mu| \geq t] \leq 2 \exp \left( -\frac{2t^2}{\sum_{j=1}^n (b_j - a_j)^2} \right).$$

**Proposition 1** (Sample Concentration Bound of D-MoCHy). *For any  $\epsilon > 0$ , if  $n \geq \frac{1}{2\epsilon^2} \ln(\frac{2}{\delta})$  and  $|\Omega| > 0$ ,  $\Pr(|C[i] - |\Omega_i|| \geq |\Omega| \cdot \epsilon) \leq \delta, \forall i \in [m]$ .*

*Proof.* Let  $t := |\Omega| \cdot \epsilon$ . Since  $\mathbb{E}[C[i]] = |\Omega_i|$  and  $X_1^i, X_2^i, \dots, X_n^i$  are independent random variables such that  $0 \leq X_j^i \leq \frac{1}{np(e, e')} = \frac{|\Omega|}{n}$  where  $j \in [n]$ , we can apply Hoeffding's inequality (Lemma 1):

$$\begin{aligned} \Pr[|C[i] - |\Omega_i|| \geq |\Omega| \cdot \epsilon] &\leq 2 \exp \left( -\frac{2\epsilon^2 |\Omega|^2}{n(|\Omega|/n)^2} \right) \\ &\leq 2 \exp(-2\epsilon^2 n) \leq \delta. \quad \square \end{aligned}$$

**Proposition 2** (Sample Concentration Bound of CODA-A). *Let  $W = \sum_{v \in V} w[v]$  and  $\bar{h} = HM(|\bar{e} \cap \bar{e}'|^2)$  be a harmonic mean of  $|\bar{e} \cap \bar{e}'|^2$  for all  $(e, e') \in \Omega$ , i.e.,  $HM(|\bar{e} \cap \bar{e}'|^2) = n / \sum_{(e, e') \in \Omega} \frac{1}{|\bar{e} \cap \bar{e}'|^2}$ . Then for any  $\epsilon > 0$ , if  $n \geq \frac{1}{2\epsilon^2 \bar{h}} \ln(\frac{2}{\delta})$  and  $W > 0$ ,  $\Pr(|C[i] - |\Omega_i|| \geq W \cdot \epsilon) \leq \delta, \forall i \in [m]$ .*

*Proof.* Let  $t := W \cdot \epsilon$ . Since  $\mathbb{E}[C[i]] = |\Omega_i|$  and  $X_1^i, X_2^i, \dots, X_n^i$  are independent random variables such that  $0 \leq X_j^i \leq \frac{1}{np(e, e')} = \frac{W}{n \cdot |\bar{e} \cap \bar{e}'|}$  where  $j \in [n]$ , we can apply Hoeffding's inequality (Lemma 1):

$$\begin{aligned} \Pr[|C[i] - |\Omega_i|| \geq W \cdot \epsilon] &\leq 2 \exp \left( -\frac{2\epsilon^2 W^2}{\sum_{(e, e') \in \Omega} \left( \frac{W}{n \cdot |\bar{e} \cap \bar{e}'|} \right)^2} \right) \\ &\leq 2 \exp(-2\epsilon^2 n \bar{h}) \leq \delta. \quad \square \end{aligned}$$

## C. A2A: Baseline Algorithm (Section V-D of the main paper)

In this section, we provide a detailed description of the baseline algorithm, A2A, including its unbiasedness, variance, and complexity. Its pseudocode is presented in Algorithm 1. Here,  $p(e, e') = \left( \frac{1}{|N_e|} + \frac{1}{|N_{e'}|} \right) \cdot \frac{1}{|E_{\geq 1}|}$  where  $E_{\geq 1} = \{e : N_e \geq 1\}$ .

Assume  $E_{\geq 1}$  is given at first. Also, for space efficiency, we assume  $N_e$  is maintained (Line 4).  $HM(A, B)$  on Line 5 denotes the harmonic mean of  $A$  and  $B$ .

---

**Algorithm 1:** A2A

---

**Input:** (1) a directed hypergraph:  $G = (V, E)$   
(2) # of samples  $n = q \cdot |E|$  for  $q \in (0, 1)$   
**Output:**  $C[i]$  for every  $i \in [m]$   
1  $C[i] \leftarrow 0, \forall i \in [m]$   
2 **for**  $1 : n$  **do**  
3     Choose  $e \in E_{\geq 1}$  uniformly at random  
4      $N_e \leftarrow \{e' \in E \setminus \{e\} : e \cap e' \neq \emptyset\}$   
5      $C[f(e, e')] \leftarrow C[f(e, e')] + \frac{|E_{\geq 1}|}{2 \cdot n} \cdot HM(|N_e|, |N_{e'}|)$   
6 **return**  $C$

---

**Proposition 3** (Unbiasedness of A2A). *Algorithm 1 is unbiased, i.e.,  $\mathbb{E}[C[i]] = |\Omega_i|$ .*

*Proof.* Follow the flow of the proof of Proposition 2.  $\square$

**Proposition 4** (Variance of A2A). *The variance of  $C[i]$  obtained by Algorithm 1 is*

$$\begin{aligned} \text{Var}[C[i]] &= \sum_{(e, e') \in \Omega_i} \frac{1}{n} \left( \frac{1}{p(e, e')} - 1 \right) \\ &= \sum_{(e, e') \in \Omega_i} \frac{1}{n} \left( \frac{|E_{\geq 1}|}{2} \cdot HM(|N_e|, |N_{e'}|) - 1 \right). \end{aligned}$$

*Proof.* Follow the flow of the proof of Proposition 3.  $\square$

**Proposition 5** (Time & Space complexity of A2A). *The time complexity of Algorithm 1 is  $O(n \cdot (\max_{e \in E} |\bar{e}| \cdot \max_{e \in E} |N_e|))$ . Its space complexity is  $O(\sum_{e \in E} |\bar{e}|)$ .*

*Proof.* The information of a given directed graph is stored in  $O(\sum_{e \in E} |\bar{e}|)$  space at first. For time complexity,  $O(\max_{e \in E} |\bar{e}| \cdot \max_{e \in E} |N_e|)$  time is required assuming  $O(p \cdot q)$  time is taken for set union when there are  $p$  sets, of which size bounded by  $q$ . For space complexity,  $O(|N_e|) \in O(\sum_{e \in E} |\bar{e}|)$  space is needed. Checking  $f(e, e')$  requires  $O(\max_{(e, e') \in \Omega} \min(|\bar{e}|, |\bar{e}'|))$ -time, which is bounded by  $O(\max_{e \in E} |\bar{e}| \cdot \max_{e \in E} |N_e|)$ .  $\square$

#### D. Count Distributions (Section V-B of the main paper)

We analyze the occurrence distributions of DHGs in real-world and randomized directed hypergraphs (DHs). To ensure statistical significance, we generate ten randomized DHs and report the average counts. As shown in Figure 1, the counts of DHGs in real-world directed hypergraphs are distinct from those in randomized directed hypergraphs.

#### E. Temporal Analysis (Section V-E of the main paper)

We analyze time-evolving DHs (all considered DHs except for the metabolic datasets, which do not contain timestamps). A time-evolving DH  $G = (V, E)$  has timestamp  $\tau_e$  for each  $e \in E$ , i.e.,  $e = \langle H, T, \tau_e \rangle$ . With regard to the citation datasets, citation-data-science consists of 41 timestamps, while citation-software includes

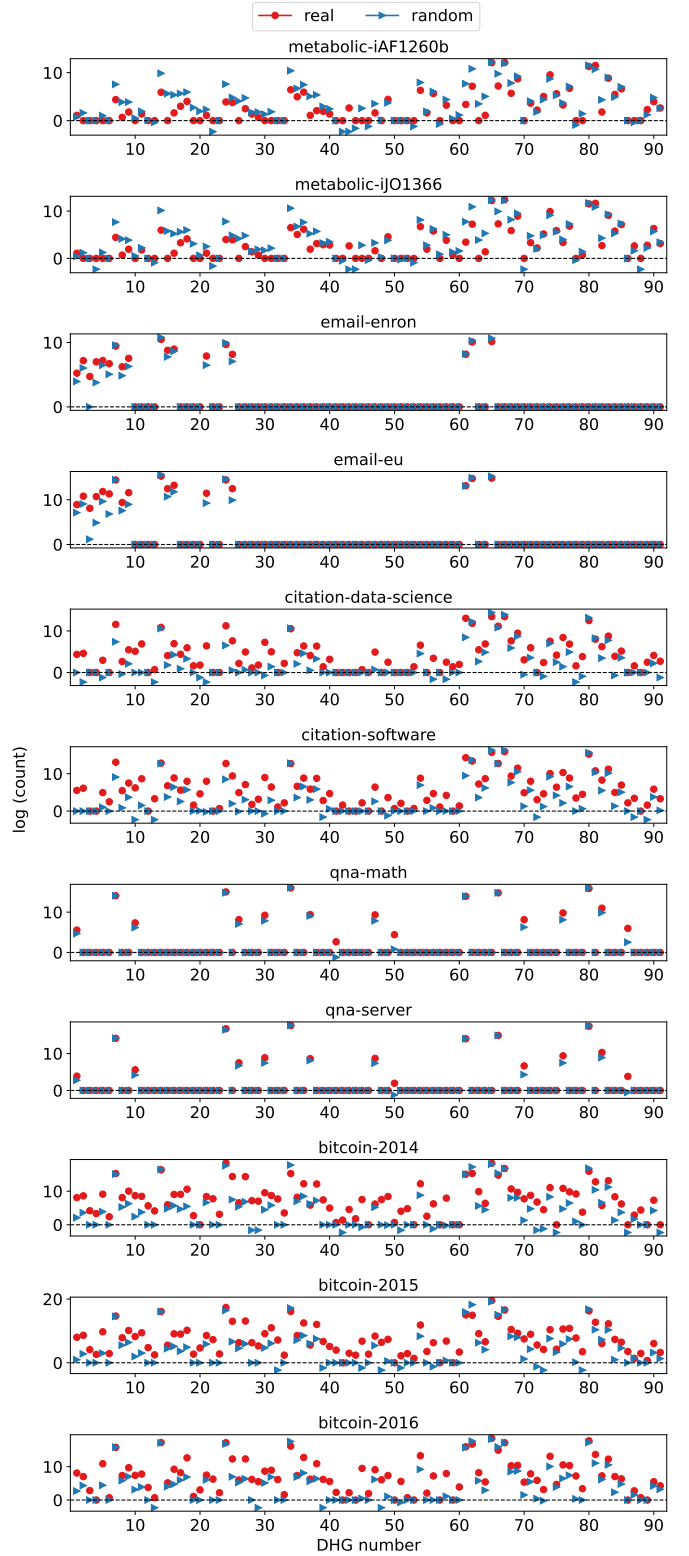


Fig. 1. Log counts of DHGs in real-world and randomized directed hypergraphs (DHs). The counts of DHGs are clearly distinguished in real-world and randomized DHs.

49 timestamps, with each publication year assigned as a timestamp. For the email, qna, and bitcoin datasets, we consider 10 timestamps  $\{t_1, t_2, \dots, t_{10}\}$  of the same interval,

where  $t_1 < \dots < t_{10} = \max_{e \in E} \tau_e$  and  $t_2 - t_1 = t_1 - \min_{e \in E} \tau_e$ . For each timestamp  $t_i$  above, we create a snapshot (i.e., sub-DH) where the edge set is  $E_i = \{e : \tau_e \leq t_i\}$  and the node set  $V_i = \bigcup_{e \in E_i} \bar{e}$ . Then, we compute the occurrence ratio of each DHG in each sub-DH.

In Figure 2, we visualize DHGs whose ratio is greater than specific thresholds while aggregating the rest as Others. The threshold values for the citation, email, qna, and bitcoin datasets are 0.03, 0.1, 0.01, and 0.03, respectively. In addition, we summarize the time-evolving patterns of the top 10 most frequent DHGs in Figure 3. Notably, the datasets from the same domain not only have the same set of frequent DHGs but also exhibit similar time-evolving tendencies for each DHG.

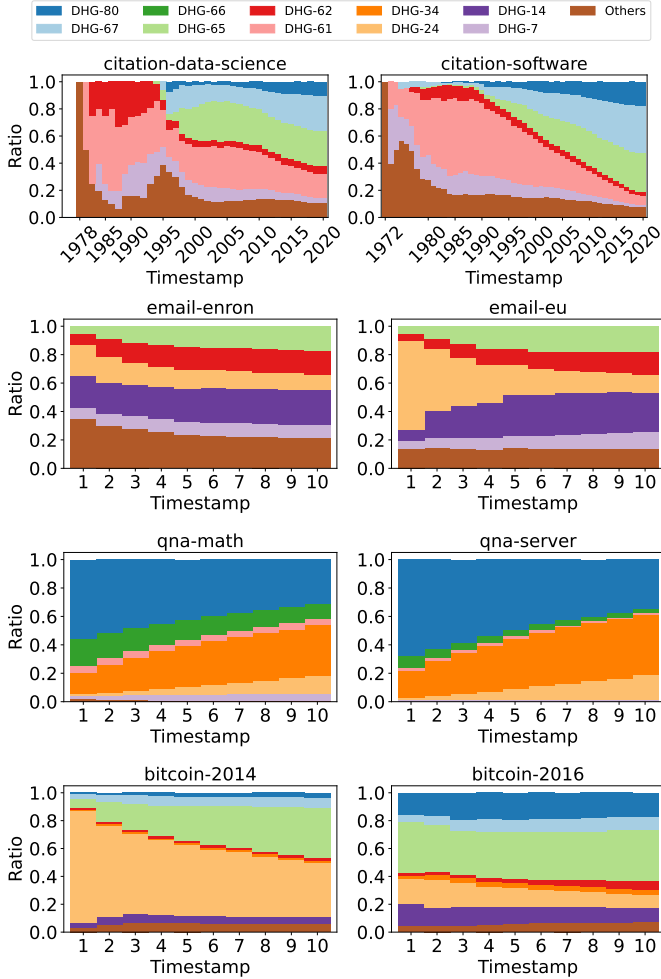


Fig. 2. Directed hypergraphs from the same domain not only share the same set of frequent DHGs but also exhibit similar time-evolving tendencies. DHGs with ratios below certain thresholds (spec., 0.03 for the citation datasets, 0.1 for the email datasets, 0.01 for the qna datasets, and 0.03 for the bitcoin datasets) are grouped as Others.

**Citation datasets:** The ratios of DHG-65, -67, and -80 increase, while those of DHG-7, -61, and -62 decrease. In DHG-65, -67, and -80, all non-intersecting regions (i.e., regions 1, 4, 5, and 8 in Figure 1(c) contain at least one node, while in

	80	67	66	65	62	61	34	24	14	7
CD/CS	↑/↑	↑/↑	X	↑/↑	↓/↓	↓/↓	X	X	X	↓/↓
EN/EU	X	X	X	↑/↑	↑/↑	X	X	↓/↓	↑/↑	↑/↑
QM/QS	↓/↓	X	↓/↓	X	X	↓/↓	↑/↑	↑/↑	X	↑/↑
B4/B6	↑/↓	↑/↑	X	↑/↑	↓/↑	X	↑/↓	↓/↓	↓/↓	X

Fig. 3. Time-evolving trend. Each row represents a domain of datasets and each column represents a DHG. DHGs marked with 'X' have ratios less than a predefined threshold. The ratios of DHGs marked with ↑ or ↓ tend to increase or decrease, respectively.

DHG-7, -61, and -62, some non-intersecting regions are empty. That is, the number of non-empty non-intersecting regions increases over time.

**Email datasets:** Among the frequent DHGs, only the ratio of DHG-24 decreases, whereas the ratios of DHG-7, -14, -62, and -65 increase. DHG-24 is distinct from the other DHGs in that two tail sets intersect in it. Given that the size of tail sets in email datasets is always 1, the probability of two hyperarcs sharing the same tail set decreases over time, resulting in the decrease of the DHG-24 ratio.

**Qna datasets:** There is a dramatic decrease in the ratio of DHG-80 and a dramatic increase in the ratio of DHG-34. The ratios of DHG-61, -66, and -80 decrease, while the ratios of DHG-7, -24, and -34 increase. The increasing DHGs have empty non-intersecting areas in their tail sets, while the declining DHGs have no such areas. This indicates that the number of users who frequently answer questions increases.

**Bitcoin datasets:** Although the two bitcoin datasets share the same set of frequent DHGs, their tendencies to increase or decrease over time differ in them. For example, DHG-65 becomes dominant in the bitcoin-2016 dataset, with a ratio of 0.37, while it has a ratio of only 0.07 in the other dataset. Conversely, DHG-24 becomes dominant in the bitcoin-2014 dataset, with a ratio of 0.81, but only has a ratio of 0.10 in the other dataset. The main difference between DHG-65 and DHG-24 is the presence or absence of an intersection between tail sets. DHG-24 has only an intersection between tail sets, but DHG-65 does not. This indicates that the diversity of accounts participating in transactions increases over time.

#### F. Experimental Settings for Hyperarc Prediction (Section V-C of the main paper)

In this section, we list the hyperparameter settings of the feature vectors and classifiers used for the hyperarc prediction and report the detailed experimental setups.

**Hyperparameter settings of feature vectors:** The embedding dimensions of node2vec, hyper2vec, and deep hyperedges are all fixed to 91. Other hyperparameters of these methods are fixed to their default settings at the following links:

- **node2vec (n2v):** <https://github.com/aditya-grover/node2vec>
- **hyper2vec (h2v):** <https://github.com/jeffhj/NHNE>
- **deep hyperedges (deep-h):** <https://github.com/0xpayne/deep-hyperedges>

Note that h-motif and triad do not have any hyperparameters.

**Details of classifiers:** The hyperparameters of the tree-based classifiers (Decision Tree, Random Forest, XGBoost, and LightGBM), Logistic Regressor, KNN, and MLP are fixed to their default settings at the following links:

- **Decision Tree (DT):** <https://scikit-learn.org/stable/modules/generated/sklearn.tree.DecisionTreeClassifier>
- **Random Forest (RF):** <https://scikit-learn.org/stable/modules/generated/sklearn.ensemble.RandomForestClassifier>
- **XGBoost (XGB):** <https://xgboost.readthedocs.io/en/stable/>
- **LightGBM (LGBM):** <https://lightgbm.readthedocs.io/en/latest/pythonapi/lightgbm.LGBMClassifier>
- **Logistic Regressor (LR):** [https://scikit-learn.org/stable/modules/generated/sklearn.linear\\_model.LogisticRegression](https://scikit-learn.org/stable/modules/generated/sklearn.linear_model.LogisticRegression)
- **KNN:** <https://scikit-learn.org/stable/modules/generated/sklearn.neighbors.KNeighborsClassifier>
- **MLP:** [https://scikit-learn.org/stable/modules/generated/sklearn.neural\\_network.MLPClassifier](https://scikit-learn.org/stable/modules/generated/sklearn.neural_network.MLPClassifier)

To utilize the hyperarc-level feature vectors for hypergraph-neural-network-based (HNN-based) classifiers (HGNN, FastHyperGCN, and UniGCNII), which assume that the input is an undirected hypergraph with node features, we use the “dual” hypergraph of a given directed hypergraph (DH) as the input of the classifiers. In the dual hypergraph  $G^* = (V^*, E^*)$  of a DH  $G = (V, E)$ , each node is a hyperarc in  $G$  (i.e.,  $V^* = E$ ) and each hyperedge is the set of hyperarcs containing a node in  $G$  (i.e.,  $E^* = \{E_v : v \in V\}$ ).

The hyperparameters of these HNN-based classifiers are set as follows: the number of layers and hidden dimension are all fixed to 2 and 128, respectively. We train HGNN and UniGCNII for 500 epochs using Adam [10] with a learning rate of 0.001 and a weight decay of  $10^{-6}$ , and FastHyperGCN for 200 epochs using Adam with a learning rate of 0.01, a weight decay of  $5 \times 10^{-4}$ , and a dropout rate of 0.5.

For these HNN-based classifiers, we employ early stopping, and to this end, we divide the fake hyperarcs into the train, validation, and test sets using a 6:2:2 ratio. In each set, we uniformly sample the same number of real hyperarcs as the number of fake hyperarcs. For every 50 epochs, we measure the validation accuracy and save the model parameters. Then, we use the checkpoint (i.e., saved model parameters) with the highest validation accuracy to measure test performance.

#### G. Application Results (Section V-C of the main paper)

In this section, we report the full results of the hyperarc prediction problem. Tables I and II report the AUROC and accuracy results (average over 100 trials). The best performances are highlighted in bold. Notably, in terms of average ranking, using DHG vectors performs best in all settings, achieving up to 33% higher AUROC on the `bitcoin-2016` dataset and a 47% higher accuracy on the `bitcoin-2014` dataset than the second best features.

#### REFERENCES

- [1] N. Yadati, V. Nitin, M. Nimishakavi, P. Yadav, A. Louis, and P. Talukdar, “Nhp: Neural hypergraph link prediction,” in *CIKM*, 2020.
- [2] P. Chodrow and A. Mellor, “Annotated hypergraphs: models and applications,” *Applied Network Science*, vol. 5, no. 1, pp. 1–25, 2020.
- [3] J. Leskovec and A. Krevl, “SNAP Datasets: Stanford large network dataset collection,” <http://snap.stanford.edu/data>, Jun. 2014.
- [4] J. Tang, J. Zhang, L. Yao, J. Li, L. Zhang, and Z. Su, “Arnetminer: Extraction and mining of academic social networks,” in *KDD*, 2008.
- [5] A. Sinha, Z. Shen, Y. Song, H. Ma, D. Eide, B.-J. Hsu, and K. Wang, “An overview of microsoft academic service (mas) and applications,” in *WWW*, 2015.
- [6] S. Kim, M. Choe, J. Yoo, and K. Shin, “Reciprocity in directed hypergraphs: Measures, findings, and generators,” in *ICDM*, 2022.
- [7] S. Exchange, “Stack exchange data dump,” <https://archive.org/details/stackexchange>, 2020.
- [8] J. Wu, J. Liu, W. Chen, H. Huang, Z. Zheng, and Y. Zhang, “Detecting mixing services via mining bitcoin transaction network with hybrid motifs,” *IEEE Trans. Syst. Man Cybern.: Syst.*, vol. 52, no. 4, pp. 2237–2249, 2021.
- [9] W. Hoeffding, “Probability inequalities for sums of bounded random variables,” *The collected works of Wassily Hoeffding*, pp. 409–426, 1994.
- [10] D. P. Kingma and J. Ba, “Adam: A method for stochastic optimization,” in *ICLR*, 2015.

TABLE I

HYPERARC PREDICTION PERFORMANCE (AUROC). WE COMPARE SIX HYPERARC FEATURE VECTORS USING TEN CLASSIFIERS, AND THE BEST PERFORMANCES ARE HIGHLIGHTED IN BOLD. NOTABLY, USING DHG VECTORS LEADS TO THE BEST (UP TO 33% BETTER) PERFORMANCE IN MOST SETTINGS, INDICATING THAT DHGS EXTRACT HIGHLY INFORMATIVE HYPERARC FEATURES.

Model	Dataset	DHG	h-motif	triad	n2v	h2v	deep-h	Dataset	DHG	h-motif	triad	n2v	h2v	deep-h
LR	MB	0.728±0.022	0.724±0.015	0.580±0.017	0.506±0.021	0.509±0.013	0.785±0.017	M6	0.721±0.016	0.727±0.020	0.622±0.012	0.501±0.015	0.504±0.013	0.795±0.010
RF		0.826±0.015	0.784±0.020	0.703±0.011	0.539±0.018	0.533±0.013	0.793±0.018		0.834±0.011	0.794±0.018	0.730±0.013	0.541±0.010	0.546±0.027	0.803±0.012
DT		0.651±0.009	0.632±0.019	0.599±0.015	0.512±0.014	0.506±0.011	0.583±0.016		0.656±0.018	0.641±0.015	0.611±0.009	0.509±0.014	0.517±0.016	0.582±0.014
KNN		0.762±0.013	0.755±0.018	0.673±0.011	0.550±0.018	0.552±0.020	0.760±0.015		0.746±0.012	0.752±0.017	0.673±0.018	0.535±0.015	0.560±0.018	0.778±0.013
MLP		0.696±0.016	0.694±0.021	0.622±0.021	0.543±0.016	0.559±0.020	0.800±0.009		0.687±0.016	0.705±0.011	0.646±0.018	0.548±0.012	0.559±0.017	0.804±0.011
XGB		0.812±0.013	0.752±0.025	0.684±0.019	0.518±0.018	0.526±0.018	0.775±0.010		0.819±0.020	0.765±0.016	0.710±0.014	0.530±0.014	0.537±0.019	0.792±0.011
LGBM		0.799±0.057	0.736±0.062	0.680±0.072	0.540±0.059	0.529±0.021	0.785±0.012		0.822±0.047	0.747±0.055	0.687±0.063	0.515±0.057	0.541±0.016	0.794±0.015
HGNN		0.594±0.060	0.554±0.059	0.541±0.067	0.479±0.058	0.506±0.086	0.522±0.060		0.601±0.062	0.551±0.049	0.552±0.052	0.509±0.051	0.526±0.027	0.534±0.043
FHGCN		0.729±0.065	0.567±0.072	0.612±0.056	0.506±0.059	0.490±0.067	0.561±0.060		0.720±0.072	0.553±0.070	0.615±0.065	0.506±0.059	0.484±0.059	0.566±0.065
UGCNII		0.680±0.060	0.674±0.048	0.641±0.097	0.488±0.049	0.489±0.068	0.607±0.092		0.663±0.058	0.663±0.044	0.647±0.056	0.502±0.045	0.503±0.035	0.642±0.043
Max		0.826±0.015	0.784±0.020	0.703±0.011	0.550±0.018	0.559±0.020	0.800±0.009		0.834±0.011	0.794±0.018	0.730±0.013	0.548±0.012	0.560±0.018	0.804±0.011
Avg.		0.728±0.075	0.687±0.080	0.634±0.052	0.518±0.024	0.520±0.024	0.697±0.113		0.727±0.079	0.690±0.086	0.649±0.053	0.520±0.017	0.528±0.025	0.709±0.113
Rank Avg.		1.200±0.422	2.700±0.483	3.500±0.707	5.600±0.516	5.400±0.516	2.600±1.265		1.600±0.966	2.600±0.699	3.400±0.843	5.900±0.316	5.100±0.316	2.400±1.265
LR	EN	0.883±0.014	0.826±0.015	0.783±0.016	0.627±0.017	0.680±0.020	0.634±0.023	EU	0.933±0.002	0.838±0.004	0.876±0.003	0.691±0.004	0.494±0.003	0.722±0.002
RF		0.880±0.016	0.856±0.010	0.773±0.021	0.684±0.024	0.624±0.029	0.623±0.024		0.960±0.002	0.921±0.003	0.901±0.003	0.737±0.003	0.529±0.004	0.770±0.004
DT		0.707±0.010	0.690±0.019	0.652±0.019	0.551±0.022	0.529±0.017	0.542±0.021		0.852±0.003	0.762±0.004	0.785±0.005	0.546±0.004	0.504±0.007	0.564±0.007
KNN		0.846±0.013	0.810±0.015	0.745±0.020	0.685±0.019	0.597±0.026	0.591±0.024		0.920±0.002	0.854±0.005	0.881±0.003	0.701±0.003	0.586±0.019	0.749±0.003
MLP		0.883±0.013	0.825±0.017	0.780±0.013	0.697±0.019	0.618±0.024	0.636±0.022		0.962±0.001	0.909±0.004	0.911±0.004	0.790±0.005	0.539±0.015	0.802±0.003
XGB		0.863±0.017	0.847±0.014	0.765±0.022	0.666±0.022	0.632±0.025	0.610±0.019		0.961±0.001	0.917±0.002	0.905±0.003	0.747±0.005	0.557±0.011	0.777±0.002
LGBM		0.842±0.056	0.847±0.060	0.769±0.063	0.655±0.081	0.635±0.027	0.612±0.027		0.963±0.005	0.923±0.006	0.908±0.008	0.761±0.014	0.555±0.007	0.796±0.002
HGNN		0.505±0.052	0.543±0.070	0.554±0.070	0.532±0.070	0.543±0.062	0.532±0.080		0.529±0.028	0.520±0.020	0.516±0.017	0.504±0.018	0.502±0.014	0.500±0.017
FHGCN		0.804±0.102	0.738±0.099	0.773±0.073	0.548±0.075	0.619±0.084	0.570±0.073		0.849±0.054	0.724±0.051	0.888±0.041	0.520±0.029	0.550±0.057	0.614±0.070
UGCNII		0.787±0.048	0.767±0.065	0.788±0.052	0.706±0.045	0.739±0.056	0.606±0.059		0.874±0.010	0.805±0.010	0.912±0.007	0.793±0.014	0.812±0.020	0.784±0.012
Max		0.883±0.014	0.856±0.010	0.788±0.052	0.706±0.045	0.739±0.056	0.636±0.022		0.963±0.005	0.923±0.006	0.788±0.052	0.706±0.045	0.739±0.056	0.802±0.003
Avg.		0.800±0.117	0.775±0.098	0.738±0.076	0.635±0.067	0.602±0.071	0.596±0.037		0.880±0.132	0.817±0.126	0.848±0.123	0.679±0.113	0.563±0.092	0.708±0.108
Rank Avg.		1.700±1.567	2.200±0.632	2.500±0.850	4.500±0.707	4.800±1.229	5.300±0.823		1.200±0.422	2.700±0.675	2.200±0.789	5.000±0.471	5.500±0.972	4.400±0.843
LR	CD	0.969±0.002	0.857±0.003	0.644±0.003	0.564±0.004	0.512±0.003	0.653±0.004	CS	0.980±0.001	0.890±0.002	0.722±0.004	0.584±0.002	0.516±0.002	0.688±0.002
RF		0.997±0.000	0.939±0.001	0.703±0.007	0.573±0.006	0.498±0.004	0.707±0.005		0.999±0.000	0.945±0.003	0.777±0.004	0.611±0.004	0.502±0.005	0.739±0.004
DT		0.963±0.001	0.777±0.007	0.583±0.006	0.511±0.004	0.497±0.003	0.539±0.004		0.974±0.001	0.783±0.011	0.623±0.004	0.519±0.003	0.498±0.004	0.548±0.002
KNN		0.962±0.002	0.857±0.004	0.629±0.008	0.595±0.005	0.520±0.010	0.633±0.005		0.974±0.001	0.899±0.002	0.702±0.004	0.632±0.003	0.531±0.011	0.659±0.002
MLP		0.990±0.001	0.914±0.007	0.693±0.009	0.597±0.006	0.510±0.005	0.776±0.003		0.996±0.000	0.930±0.004	0.775±0.005	0.671±0.006	0.544±0.014	0.806±0.002
XGB		0.997±0.000	0.937±0.002	0.703±0.008	0.579±0.004	0.507±0.007	0.747±0.004		0.999±0.000	0.939±0.005	0.781±0.004	0.620±0.004	0.522±0.007	0.786±0.002
LGBM		0.998±0.001	0.941±0.008	0.719±0.021	0.587±0.014	0.511±0.004	0.782±0.003		0.999±0.000	0.946±0.017	0.792±0.012	0.626±0.019	0.525±0.005	0.807±0.001
HGNN		0.629±0.008	0.528±0.017	0.523±0.013	0.537±0.014	0.540±0.022	0.510±0.013		0.587±0.006	0.509±0.023	0.510±0.012	0.562±0.009	0.590±0.012	0.508±0.007
FHGCN		0.861±0.009	0.700±0.053	0.637±0.060	0.516±0.028	0.513±0.021	0.505±0.011		0.852±0.044	0.718±0.050	0.714±0.054	0.513±0.025	0.511±0.024	0.505±0.013
UGCNII		0.975±0.005	0.874±0.010	0.714±0.013	0.851±0.016	0.672±0.042	0.547±0.012		0.971±0.003	0.812±0.010	0.792±0.011	0.899±0.016	0.895±0.007	0.609±0.015
Max		0.998±0.001	0.941±0.008	0.719±0.021	0.851±0.016	0.672±0.042	0.782±0.003		0.999±0.000	0.946±0.017	0.792±0.012	0.899±0.016	0.895±0.007	0.807±0.001
Avg.		0.934±0.115	0.832±0.132	0.655±0.064	0.591±0.096	0.528±0.052	0.640±0.110		0.933±0.129	0.837±0.139	0.719±0.091	0.624±0.109	0.563±0.119	0.666±0.119
Rank Avg.		1.000±0.000	2.200±0.632	3.900±0.568	4.500±0.850	5.400±1.265	4.000±1.414		1.100±0.316	2.500±1.080	3.600±0.699	4.400±1.075	5.100±1.729	4.300±1.252
LR	QM	0.652±0.003	0.620±0.004	0.580±0.004	0.499±0.003	0.514±0.003	0.600±0.002	QS	0.598±0.001	0.553±0.002	0.558±0.003	0.512±0.001	0.528±0.002	0.586±0.002
RF		0.734±0.003	0.657±0.006	0.663±0.006	0.505±0.003	0.504±0.004	0.767±0.005		0.728±0.001	0.595±0.002	0.637±0.003	0.501±0.003	0.504±0.003	0.748±0.002
DT		0.621±0.003	0.547±0.006	0.569±0.004	0.502±0.001	0.502±0.004	0.547±0.004		0.630±0.002	0.524±0.002	0.571±0.003	0.500±0.002	0.501±0.002	0.545±0.002
KNN		0.638±0.002	0.601±0.004	0.570±0.003	0.506±0.003	0.511±0.006	0.561±0.002		0.669±0.002	0.552±0.003	0.599±0.002	0.505±0.003	0.503±0.004	0.610±0.002
MLP		0.737±0.004	0.649±0.005	0.634±0.003	0.514±0.004	0.509±0.002	0.834±0.004		0.717±0.002	0.573±0.002	0.630±0.002	0.511±0.002	0.525±0.004	0.815±0.001
XGB		0.744±0.003	0.660±0.005	0.677±0.005	0.504±0.003	0.513±0.004	0.823±0.002		0.745±0.001	0.612±0.002	0.653±0.003	0.504±0.002	0.507±0.002	0.801±0.002
LGBM		0.755±0.010	0.679±0.016	0.694±0.015	0.505±0.014	0.513±0.003	0.844±0.002		0.753±0.005	0.628±0.014	0.669±0.018	0.506±0.009	0.513±0.003	0.813±0.002
HGNN		0.570±0.013	0.520±0.011	0.535±0.012	0.519±0.012	0.566±0.009	0.551±0.010		0.619±0.008	0.543±0.006	0.563±0.006	0.534±0.008	0.599±0.007	0.583±0.009
FHGCN		0.538±0.031	0.507±0.010	0.545±0.044	0.501±0.005	0.507±0.020	0.521±0.028		0.593±0.041	0.528±0.025	0.546±0.049	0.502±0.007	0.503±0.012	0.511±0.018
UGCNII		0.658±0.007	0.620±0.011	0.642±0.011	0.661±0.012	0.689±0.007	0.817±0.014		0.713±0.005	0.636±0.008	0.649±0.007	0.594±0.010	0.713±0.006	0.824±0.008
Max		0.755±0.010	0.679±0.016	0.694±0.015	0.661±0.012	0.689±0.007	0.844±0.002		0.753±0.005	0.636±0.008	0.669±0.018	0.594±0.010	0.713±0.006	0.824±0.008
Avg.		0.665±0.076	0.606±0.061	0.611±0.058	0.522±0.049	0.533±0.058	0.687±0.140		0.677±0.062	0.574±0.041	0.608±0.045	0.517±0.029	0.540±0.068	0.684±0.127
Rank Avg.		1.800±0.919	3.800±1.317	3.200±1.135	5.500±0.972	4.500±1.434	2.200±1.317		1.700±0.949	4.100±0.568	2.900±0.568	5.900±0.316	4.500±1.354	1.900±1.101
LR	B4	0.693±0.003	O.O.T.*	0.616±0.001	0.569±0.001	0.559±0.000	0.640±0.000	B5	0.696±0.002	O.O.T.*	0.612±0.003	0.592±0.001	0.563±0.001	0.627±0.001
RF		0.776±0.001	O.O.T.*	0.799±0.009	0.562±0.003	0.524±0.003	0.729±07							

TABLE II

HYPERARC PREDICTION PERFORMANCE (ACCURACY). WE COMPARE SIX HYPERARC FEATURE VECTORS USING TEN CLASSIFIERS, AND THE BEST PERFORMANCES ARE HIGHLIGHTED IN BOLD. NOTABLY, USING DHG VECTORS LEADS TO THE BEST (UP TO 47% BETTER) PERFORMANCE IN MOST SETTINGS, INDICATING THAT DHGS EXTRACT HIGHLY INFORMATIVE HYPERARC FEATURES.

Model	Dataset	DHG	h-motif	triad	n2v	h2v	deep-h	Dataset	DHG	h-motif	triad	h2v	h2v	h2v	deep-h
LR	MB	0.656±0.023	0.649±0.015	0.549±0.018	0.504±0.017	0.511±0.012	<b>0.701±0.014</b>	M6	0.656±0.016	0.648±0.019	0.584±0.011	0.506±0.011	0.505±0.011	<b>0.713±0.012</b>	
RF		0.690±0.011	0.681±0.021	0.650±0.009	0.531±0.014	0.518±0.012	<b>0.714±0.015</b>		0.698±0.014	0.704±0.017	0.666±0.010	0.532±0.010	0.527±0.015	<b>0.723±0.017</b>	
DT		<b>0.651±0.009</b>	0.632±0.019	0.597±0.016	0.512±0.014	0.506±0.011	0.583±0.016		<b>0.656±0.018</b>	0.641±0.015	0.612±0.009	0.509±0.014	0.517±0.016	0.582±0.014	
KNN		0.696±0.014	0.696±0.018	0.625±0.014	0.537±0.014	0.534±0.016	<b>0.704±0.014</b>		0.682±0.014	0.691±0.020	0.628±0.019	0.520±0.016	0.539±0.011	<b>0.725±0.013</b>	
MLP		0.654±0.011	0.646±0.014	0.603±0.019	0.533±0.008	0.537±0.014	<b>0.705±0.014</b>		0.656±0.012	0.653±0.008	0.618±0.015	0.537±0.009	0.539±0.011	<b>0.710±0.012</b>	
XGB		<b>0.708±0.016</b>	0.666±0.024	0.625±0.015	0.514±0.016	0.519±0.015	0.695±0.015		<b>0.709±0.022</b>	0.681±0.017	0.657±0.013	0.519±0.017	0.522±0.013	0.703±0.014	
LGBM		0.697±0.062	0.658±0.053	0.626±0.063	0.527±0.054	0.516±0.012	<b>0.698±0.012</b>		<b>0.720±0.057</b>	0.663±0.056	0.632±0.058	0.509±0.050	0.530±0.011	0.702±0.014	
HGNN		<b>0.549±0.055</b>	0.543±0.040	0.538±0.063	0.483±0.045	0.498±0.067	0.526±0.057		<b>0.569±0.055</b>	0.553±0.036	0.550±0.043	0.499±0.056	0.522±0.037	0.545±0.036	
FHGCN		<b>0.666±0.067</b>	0.535±0.051	0.555±0.055	0.507±0.045	0.491±0.059	0.538±0.050		<b>0.653±0.071</b>	0.532±0.053	0.566±0.059	0.504±0.045	0.498±0.048	0.548±0.060	
UGCNII		0.618±0.061	<b>0.625±0.038</b>	0.596±0.069	0.491±0.050	0.494±0.054	0.597±0.070		0.621±0.051	0.616±0.048	0.610±0.050	0.518±0.047	0.514±0.034	<b>0.633±0.035</b>	
Max		0.708±0.016	0.696±0.018	0.650±0.009	0.537±0.014	0.537±0.014	<b>0.714±0.015</b>		0.720±0.057	0.704±0.017	0.666±0.010	0.537±0.009	0.539±0.011	<b>0.725±0.013</b>	
Avg.	<b>0.659±0.047</b>	0.633±0.054	0.596±0.038	0.514±0.018	0.512±0.016	0.646±0.076	<b>0.662±0.044</b>	0.638±0.057	0.612±0.037	0.515±0.012	0.521±0.013	0.658±0.074			
Rank Avg.	<b>1.600±0.516</b>	2.700±0.823	3.600±0.699	5.500±0.527	5.500±0.527	2.100±1.287		<b>1.700±0.823</b>	2.700±0.675	3.600±0.699	5.600±0.516	5.400±0.516	2.000±1.247		
LR	EN	<b>0.804±0.014</b>	0.752±0.011	0.732±0.017	0.578±0.017	0.492±0.012	0.590±0.018	EU	<b>0.869±0.001</b>	0.776±0.005	0.837±0.004	0.618±0.008	0.496±0.003	0.659±0.006	
RF		<b>0.796±0.013</b>	0.773±0.017	0.712±0.023	0.626±0.024	0.562±0.024	0.592±0.022		<b>0.907±0.003</b>	0.838±0.004	0.839±0.003	0.652±0.003	0.515±0.002	0.668±0.005	
DT		<b>0.705±0.011</b>	0.689±0.018	0.654±0.020	0.551±0.022	0.528±0.018	0.542±0.021		<b>0.849±0.003</b>	0.761±0.005	0.787±0.005	0.546±0.004	0.504±0.007	0.564±0.007	
KNN		<b>0.778±0.014</b>	0.737±0.016	0.694±0.019	0.636±0.020	0.571±0.017	0.567±0.022		<b>0.875±0.002</b>	0.780±0.005	0.838±0.005	0.573±0.002	0.556±0.012	0.677±0.003	
MLP		<b>0.805±0.014</b>	0.751±0.011	0.731±0.013	0.639±0.021	0.551±0.018	0.588±0.023		<b>0.906±0.003</b>	0.821±0.007	0.857±0.005	0.660±0.016	0.507±0.005	0.675±0.011	
XGB		<b>0.775±0.018</b>	0.763±0.014	0.709±0.026	0.614±0.020	0.579±0.018	0.577±0.020		<b>0.903±0.003</b>	0.831±0.005	0.854±0.005	0.654±0.005	0.522±0.005	0.656±0.003	
LGBM		0.756±0.059	<b>0.763±0.056</b>	0.709±0.060	0.609±0.064	0.580±0.018	0.581±0.019		<b>0.906±0.010</b>	0.839±0.010	0.856±0.011	0.645±0.027	0.512±0.003	0.645±0.005	
HGNN		0.499±0.049	<b>0.543±0.063</b>	0.538±0.074	0.513±0.055	0.526±0.048	0.512±0.058		<b>0.529±0.020</b>	0.523±0.020	0.520±0.015	0.512±0.018	0.505±0.014	0.513±0.017	
FHGCN		0.693±0.117	0.651±0.090	<b>0.703±0.101</b>	0.536±0.061	0.566±0.076	0.550±0.069		0.742±0.072	0.638±0.060	<b>0.790±0.136</b>	0.512±0.020	0.519±0.038	0.547±0.054	
UGCNII		0.710±0.050	0.708±0.065	<b>0.727±0.046</b>	0.673±0.045	0.689±0.055	0.582±0.051		0.783±0.013	0.726±0.009	<b>0.859±0.008</b>	0.724±0.014	0.740±0.020	0.706±0.013	
Max		<b>0.805±0.014</b>	0.773±0.017	0.732±0.017	0.673±0.045	0.689±0.055	0.592±0.022		<b>0.907±0.003</b>	0.839±0.010	0.859±0.008	0.724±0.014	0.740±0.020	0.706±0.013	
Avg.	<b>0.732±0.092</b>	0.713±0.071	0.691±0.058	0.598±0.051	0.564±0.052	0.568±0.026	<b>0.827±0.119</b>	0.753±0.102	0.804±0.103	0.610±0.071	0.538±0.073	0.631±0.065			
Rank Avg.	<b>1.800±1.549</b>	2.000±0.667	2.500±0.850	4.400±0.699	5.100±1.101	5.200±0.632		<b>1.200±0.422</b>	3.000±0.471	1.900±0.568	5.100±0.316	5.600±0.966	4.200±0.632		
LR	CD	<b>0.921±0.004</b>	0.751±0.009	0.602±0.004	0.527±0.004	0.504±0.002	0.593±0.007	CS	<b>0.919±0.002</b>	0.767±0.002	0.662±0.005	0.541±0.005	0.508±0.005	0.625±0.007	
RF		<b>0.977±0.001</b>	0.855±0.004	0.644±0.007	0.548±0.003	0.500±0.003	0.599±0.005		<b>0.984±0.001</b>	0.866±0.006	0.702±0.006	0.568±0.005	0.501±0.003	0.621±0.005	
DT		<b>0.963±0.001</b>	0.777±0.007	0.583±0.006	0.511±0.004	0.497±0.003	0.539±0.004		<b>0.974±0.001</b>	0.783±0.011	0.623±0.004	0.519±0.003	0.498±0.004	0.548±0.002	
KNN		<b>0.917±0.003</b>	0.787±0.005	0.594±0.007	0.558±0.004	0.514±0.006	0.592±0.003		<b>0.941±0.001</b>	0.834±0.002	0.652±0.004	0.578±0.003	0.521±0.008	0.606±0.001	
MLP		<b>0.969±0.001</b>	0.822±0.008	0.637±0.008	0.545±0.006	0.502±0.004	0.633±0.008		<b>0.980±0.001</b>	0.844±0.008	0.699±0.006	0.575±0.009	0.512±0.006	0.652±0.012	
XGB		<b>0.975±0.001</b>	0.843±0.005	0.639±0.007	0.547±0.004	0.505±0.004	0.618±0.006		<b>0.984±0.001</b>	0.850±0.009	0.704±0.006	0.562±0.006	0.506±0.003	0.636±0.006	
LGBM		<b>0.977±0.004</b>	0.849±0.020	0.652±0.022	0.546±0.020	0.504±0.003	0.601±0.006		<b>0.984±0.002</b>	0.860±0.032	0.713±0.016	0.566±0.028	0.502±0.002	0.622±0.007	
HGNN		<b>0.595±0.009</b>	0.543±0.015	0.534±0.013	0.542±0.012	0.535±0.017	0.519±0.013		0.555±0.007	0.534±0.011	0.529±0.008	0.553±0.009	<b>0.568±0.009</b>	0.521±0.006	
FHGCN		<b>0.754±0.091</b>	0.597±0.087	0.556±0.067	0.505±0.015	0.504±0.013	0.502±0.008		<b>0.738±0.098</b>	0.609±0.086	0.594±0.089	0.503±0.013	0.502±0.009	0.503±0.009	
UGCNII		<b>0.932±0.005</b>	0.798±0.013	0.657±0.012	0.769±0.016	0.630±0.028	0.541±0.011		<b>0.917±0.006</b>	0.739±0.010	0.718±0.010	0.827±0.016	0.823±0.009	0.578±0.012	
Max		<b>0.977±0.001</b>	0.855±0.004	0.657±0.012	0.769±0.016	0.630±0.028	0.633±0.008		<b>0.984±0.002</b>	0.866±0.006	0.718±0.010	0.827±0.016	0.823±0.009	0.652±0.012	
Avg.	<b>0.898±0.126</b>	0.762±0.107	0.610±0.043	0.560±0.075	0.520±0.040	0.574±0.045	<b>0.898±0.142</b>	0.769±0.114	0.660±0.062	0.579±0.091	0.544±0.100	0.591±0.051			
Rank Avg.	<b>1.000±0.000</b>	2.000±0.000	3.300±0.675	4.500±0.850	5.600±0.699	4.600±0.966		<b>1.100±0.316</b>	2.400±0.843	3.400±0.843	4.400±1.075	5.200±1.751	4.500±0.850		
LR	QM	<b>0.604±0.003</b>	0.579±0.004	0.553±0.003	0.500±0.001	0.504±0.001	0.566±0.002	QS	<b>0.561±0.002</b>	0.533±0.003	0.530±0.003	0.502±0.001	0.509±0.002	0.556±0.002	
RF		<b>0.673±0.003</b>	0.613±0.005	0.620±0.004	0.503±0.003	0.502±0.003	0.581±0.005		<b>0.661±0.001</b>	0.565±0.002	0.590±0.002	0.500±0.002	0.503±0.001	0.565±0.004	
DT		<b>0.617±0.003</b>	0.547±0.006	0.572±0.004	0.502±0.001	0.502±0.004	0.547±0.004		<b>0.626±0.002</b>	0.528±0.002	0.572±0.003	0.500±0.002	0.501±0.002	0.545±0.002	
KNN		<b>0.601±0.002</b>	0.576±0.003	0.553±0.003	0.504±0.002	0.506±0.004	0.523±0.001		<b>0.619±0.002</b>	0.538±0.002	0.566±0.002	0.504±0.002	0.502±0.003	0.576±0.001	
MLP		<b>0.679±0.002</b>	0.598±0.004	0.590±0.002	0.505±0.002	0.503±0.002	0.611±0.011		<b>0.668±0.001</b>	0.544±0.003	0.603±0.003	0.509±0.002	0.506±0.003	0.598±0.013	
XGB		<b>0.681±0.002</b>	0.607±0.005	0.629±0.003	0.502±0.002	0.508±0.002	0.601±0.004		<b>0.679±0.001</b>	0.575±0.002	0.612±0.003	0.503±0.001	0.503±0.001	0.585±0.005	
LGBM		<b>0.690±0.009</b>	0.618±0.019	0.641±0.012	0.504±0.009	0.506±0.002	0.577±0.005		<b>0.688±0.004</b>	0.585±0.011	0.624±0.013	0.504±0.006	0.503±0.002	0.567±0.005	
HGNN		<b>0.549±0.011</b>	0.525±0.011	0.529±0.008	0.520±0.011	0.546±0.007	0.545±0.008		<b>0.579±0.006</b>	0.539±0.005	0.546±0.005	0.535±0.007	0.572±0.006	0.571±0.005	
FHGCN		0.512±0.022	0.503±0.007	<b>0.516±0.029</b>	0.500±0.003	0.502±0.008	0.507±0.016		<b>0.530±0.041</b>	0.505±0.014	0.515±0.027	0.501±0.003	0.501±0.005	0.502±0.009	
UGCNII		0.607±0.006	0.583±0.009	0.599±0.010	0.615±0.010	0.637±0.008	<b>0.743±0.013</b>		0.645±0.005	0.595±0.007	0.605±0.005	0.563±0.005	0.653±0.006	<b>0.752±0.007</b>	
Max		0.690±0.009	0.618±0.019	0.641±0.012	0.615±0.010	0.637±0.008	<b>0.743±0.013</b>		0.645±0.005	0.595±0.007	0.624±0.013	0.563±0.005	0.653±0.006	<b>0.752±0.007</b>	
Avg.	<b>0.621±0.060</b>	0.575±0.039	0.580±0.043	0.516±0.035	0.522±0.043	0.580±0.066	<b>0.626±0.053</b>	0.551±0.028	0.576±0.037	0.512±0.021	0.525±0.050	0.582±0.065			
Rank Avg.	<b>1.400±0.966</b>	3.400±1.265	2.900±1.287	5.500±0.972	4.600±1.430	3.200±1.033		<b>1.100±0.316</b>	3.900±0.738	2.700±0.949	5.600±0.516	4.900±1.370	2.800±0.919		